

# Figure of Merit and Cycling Sidebands in Adiabatic Decoupling

ĚRIKS KUPĀE,\* RAY FREEMAN,† GERHARD WIDER,‡ AND KURT WÜTHRICH‡

\*Varian NMR Instruments, 28 Manor Road, Walton-on-Thames, Surrey, KT12 2QF, England; †Department of Chemistry, Cambridge University, Lensfield Road, Cambridge CB2 1EW, England; and ‡Institut für Molekularbiologie und Biophysik, ETH Honggerberg, CH-8093 Zürich, Switzerland

Received March 14, 1996

Techniques for heteronuclear broadband decoupling have improved enormously over the three decades since noise decoupling was first introduced (1), initially through various forms of composite-pulse decoupling (2–7) and more recently with methods based on adiabatic fast passage (8–15). The principal aim is to increase the effective decoupling bandwidth  $\Delta F^*$  without increasing the radiofrequency power dissipation in the sample. In order to be able to compare different schemes, it is useful to define a figure of merit that measures decoupling “efficiency” in some rational manner. Since the effective bandwidth achieved by decoupling with noise or composite pulses is linearly proportional to the radiofrequency intensity  $B_2$ , the figure of merit in common use has been

$$\Xi = \frac{\Delta F^*}{(\gamma B_2/2\pi)}. \quad [1]$$

This dimensionless parameter has served its purpose well for these “hard-pulse” methods of decoupling. Noise decoupling (1) delivers a figure of merit  $\Xi = 0.3$ , WALTZ-16 (6) achieves the value  $\Xi = 1.8$ , and GARP (7) gives  $\Xi = 4.8$ . However, when we analyze the performance of adiabatic pulses, we find that the effective bandwidth increases as the square of the radiofrequency intensity  $B_2$  rather than linearly, so that  $\Xi$  cannot readily be used to compare different adiabatic schemes. This is unfortunate because the effectiveness of adiabatic decoupling depends on optimizing several instrumental parameters.

We propose to define a new figure of merit for adiabatic decoupling in terms of effective bandwidth divided by the mean radiofrequency power

$$\Phi = \frac{\Delta F^* J_{IS}}{[\gamma B_2(\text{RMS})/2\pi]^2}, \quad [2]$$

where  $B_2(\text{RMS})$  is the constant radiofrequency intensity that would have the same power dissipation as the actual amplitude-modulated  $B_2$  field. The inclusion of  $J_{IS}$  allows for the fact (discussed below) that decoupling becomes proportion-

ately more difficult as  $J_{IS}$  increases. If all the frequencies are expressed in hertz, this form of  $\Phi$  is dimensionless and on the order of unity. The original figure of merit  $\Xi$  would of course be retained for noise or composite-pulse decoupling.

Spin inversion is achieved if the sweep rate satisfies the adiabatic condition,

$$|d\theta/dt| \ll \gamma B_{\text{eff}}, \quad [3]$$

where  $B_{\text{eff}}$  is the effective radiofrequency field, determined by  $B_2$  and the offset  $\Delta B$ , and  $\theta$  is the inclination of this effective field with respect to the  $x$  axis of the rotating frame. It is usual to define an adiabaticity parameter (16) that, in principle, should be large compared with unity:

$$Q(t) = \gamma B_{\text{eff}}/|d\theta/dt|. \quad [4]$$

The rate  $d\theta/dt$  is a function of both the sweep rate, the radiofrequency intensity  $B_2$ , and the offset from resonance  $\Delta B$ . Then the formula for adiabaticity becomes (16)

$$Q(t) = \frac{\gamma(B_2^2 + \Delta B^2)^{3/2}}{|B_2(d\Delta B/dt) - \Delta B(dB_2/dt)|}. \quad [5]$$

The critical stage of any adiabatic sweep is the point where  $B_2$  sweeps through resonance for a given chemical species, so putting  $\Delta B = 0$  we obtain

$$Q_0 = \frac{\gamma B_2^2}{(d\Delta B/dt)}. \quad [6]$$

If we restrict the analysis to a linear frequency sweep, then

$$\frac{d\Delta B}{dt} = \frac{2\pi\Delta F}{\gamma T}, \quad [7]$$

where  $\Delta F$  is the total sweep range and  $T$  the duration of the sweep. In the adiabatic decoupling schemes of interest here, the radiofrequency field  $B_2$  is at its maximum level,  $B_2(\text{max})$ , at resonance. Thus,

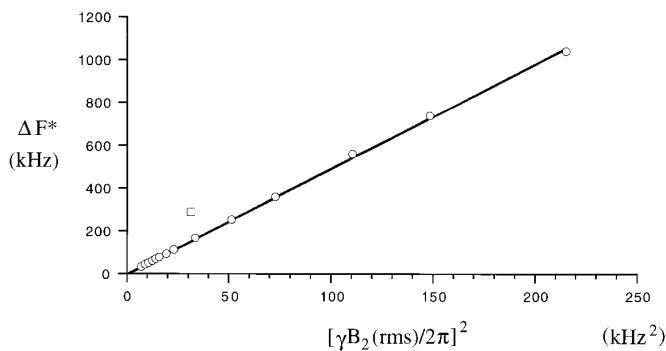


**FIG. 1.** Experimental effective bandwidths  $\Delta F^*$  recorded for WURST decoupling plotted as a function of the square of the mean radiofrequency level,  $[\gamma B_2(\text{RMS})/2\pi]^2$ . The proton signal of  $^{13}\text{C}$ -enriched sodium formate ( $J_{\text{CH}} = 200$  Hz) was observed at 500 MHz, while the  $^{13}\text{C}$  signal was decoupled. A 20-step phase cycle was used (see text). The sweep duration ( $T = 1$  ms) and the adiabaticity factor ( $Q_0 = 1.2$ ) were held constant; the other instrumental parameters are indicated in Table 1. The abnormally high bandwidth represented by the square arises from a reoptimization of the parameters with respect to the 151 Hz coupling in methyl iodide.

$$Q_0 = \frac{\{\gamma B_2(\text{max})\}^2 T}{2\pi \Delta F}. \quad [8]$$

We now introduce a quality factor  $\xi = \Delta F^*/\Delta F$ , the ratio of effective bandwidth to total sweep range, and a power factor  $f = B_2(\text{RMS})/B_2(\text{max})$ , which takes account of the fact that the radiofrequency level is brought smoothly to zero at the extremities of the sweep. Both  $\xi$  and  $f$  are numbers less than unity; for efficient decoupling schemes, they are close to unity. It follows that the effective bandwidth varies as the square of the mean radiofrequency level:

$$\Delta F^* = \frac{\xi \{\gamma B_2(\text{RMS})\}^2 T}{2\pi Q_0 f^2}. \quad [9]$$

This dependence of effective bandwidth on the radiofrequency *power* (rather than the radiofrequency *intensity*) is confirmed by experiments to decouple  $^{13}\text{C}$  from protons in enriched sodium formate ( $^1J_{\text{CH}} = 200$  Hz) in solution in heavy water. The measurements were carried out on a Varian Unity-500 spectrometer and employed a sweep duration  $T = 1$  ms, and an adiabaticity factor  $Q_0 = 1.2$ . The 20-step phase cycle was constructed from the  $(0^\circ, 150^\circ, 60^\circ, 150^\circ, 0^\circ)$  cycle of Tycko *et al.* (17) nested within the  $(0^\circ, 0^\circ, 180^\circ, 180^\circ)$  cycle of Levitt and Freeman (2). Figure 1 shows the experimentally observed decoupling bandwidths  $\Delta F^*$  plotted as a function of the square of the mean radiofrequency intensity,  $[\gamma B_2(\text{RMS})/2\pi]^2$ . There is an obvious linear relationship. Figure 2 shows that an effective bandwidth in excess of 1 MHz can be covered at the highest setting of  $B_2(\text{RMS})$ , entailing a sweep rate of over 1 GHz  $\text{s}^{-1}$ . A more realistic radiofrequency level,  $\gamma B_2(\text{RMS})/2\pi$

$= 3$  kHz, delivers an effective bandwidth of 44 kHz, which easily covers the entire range of  $^{13}\text{C}$  chemical shifts in any present-day high-resolution spectrometer.

The most serious practical limitation on broadband decoupling at high figures of merit is the introduction of cycling sidebands into the decoupled spectrum (18). These are more obtrusive if the adiabatic condition is not properly fulfilled (low  $Q_0$ ) and if the pulse repetition rate is insufficiently high in comparison with the coupling constant (13). This is why it is easier to achieve a wide effective bandwidth if the coupling constant  $J_{\text{IS}}$  is small. This is quantified in terms of a parameter

$$m = 1/(J_{\text{IS}}T), \quad [10]$$

where  $m$  is a small positive number, usually between 4 and 6. The sweep rate is therefore a compromise between two requirements—it must be slow enough to satisfy the adiabatic condition and a fast enough so that  $J_{\text{IS}}T \approx 0.2$ .

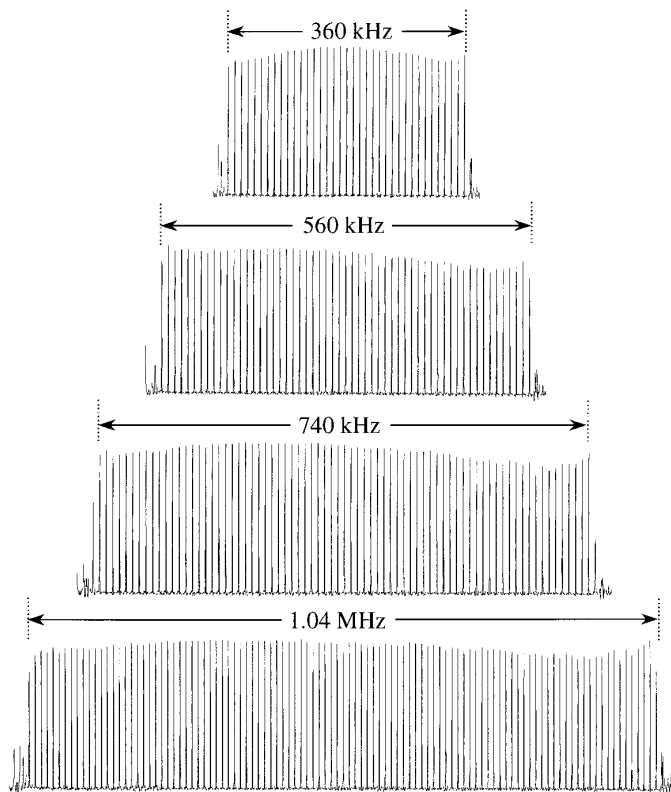


**FIG. 2.** Experimental offset dependence of WURST decoupling in  $^{13}\text{C}$ -enriched sodium formate, showing results corresponding to the last four points of Fig. 1: (a)  $\gamma B_2(\text{RMS})/2\pi = 8.5$  kHz, (b)  $\gamma B_2(\text{RMS})/2\pi = 10.5$  kHz, (c)  $\gamma B_2(\text{RMS})/2\pi = 12.2$  kHz, (d)  $\gamma B_2(\text{RMS})/2\pi = 14.3$  kHz. The fixed parameters were  $T = 1$  ms,  $m = 5$ ,  $Q_0 = 1.2$ , with  $J = 200$  Hz. The variations in the height of the decoupled line are probably attributable more to limitations in the radiofrequency circuitry at these very high bandwidths than to changes in decoupling efficiency.

We may now rewrite  $\Phi$  in terms of the practical parameters, substituting Eq. [9] in Eq. [2]:

$$\Phi = \frac{2\pi\xi J_{\text{IS}}T}{Q_0 f^2} = \frac{2\pi\xi}{mQ_0 f^2}. \quad [11]$$

This expression acts as a guide to the optimization of decoupling performance by choosing the most suitable instrumental settings. First of all, we decide on the permissible radiofrequency power, which is proportional to  $[B_2(\text{RMS})]^2$ . We then ensure that the sweep duration  $T$  is short enough that several complete adiabatic sweeps are made in a time of  $1/(J_{\text{IS}})$ ; this usually means that the parameter  $m$  is about 4 or 5; otherwise, the cycling sidebands become too obtrusive. At the same time, we adjust the relationship of the sweep rate to  $B_2(\text{max})$  so that the adiabaticity factor  $Q_0$  is low, but not so low that the adiabaticity condition is violated. It is important to maintain the adiabatic condition over a wide fraction of the sweep range  $\Delta F^*/\Delta F$ ; this implies that a broad central section of the sweep should have a constant sweep rate and a uniform radiofrequency intensity. For WURST decoupling (11, 13, 15), this requires a reasonably high index  $n$  in the expression for the pulse envelope:

$$B_2(t) = B_2(\text{max})\{1 - |\sin(\beta t)|^n\}. \quad [12]$$

This is a compromise setting, because the larger  $n$ , the nearer the power factor  $f$  approaches unity, whereas Eq. [11] implies that we should employ a *low* power factor, provided that this does not increase the peak radiofrequency to the point that the probe capacitors might break down. Note that for wide sweep ranges the appropriate setting of  $n$  becomes proportionately larger.

For the instrumental parameters used to obtain the results of Fig. 1, we find that  $\Phi$  varies only within the range 0.96 to 1.02 for the sodium formate sample ( $J_{\text{IS}} = 200$  Hz). Thus,  $\Phi = 1$  is a reasonable value for routine decoupling experiments, but it is by no means the largest possible figure of merit. Experiments previously reported (15) set out to “sail close to the wind” in order to achieve a very high bandwidth for a given radiofrequency power. The sample was enriched methyl iodide ( $J_{\text{CH}} = 151$  Hz) and the instrumental parameters were  $\gamma B_2(\text{RMS})/2\pi = 5.6$  kHz,  $T = 1.5$  ms,  $n = 240$ , and  $Q_0 = 1$ , yielding a bandwidth of 290 kHz, corresponding to a relatively high figure of merit  $\Phi = 1.40$  (Fig. 1). Note that these experiments employed very high values for  $\xi$ ,  $f$ , and  $n$  (Table 1), typical of situations where a high figure of merit is the prime concern. An example of a very small coupling ( $J_{\text{PH}} = 11$  Hz) is provided by  $\{^{31}\text{P}\}$ H decoupling in trimethyl phosphite (15), where the pulse duration can be increased to 15 ms and the mean radiofrequency level reduced to 0.92 kHz. This gives an effective decoupling bandwidth of 66 kHz and a figure of merit  $\Phi = 0.86$ .

**TABLE 1**  
Effective Bandwidths  $\Delta F^*$  and Figures of Merit  $\Phi$  for WURST Decoupling with  $J = 200$  Hz,  $Q_0 = 1.2$  and  $T = 1.0$  ms

$\gamma B_2(\text{RMS})/2\pi$ (kHz)	$\xi^a$	$f^b$	$n^c$	$\Delta F^*$ (kHz)	$\Phi$
2.67	0.68	0.77	20	34	0.96
2.98	0.73	0.79	25	44	1.00
3.25	0.74	0.81	30	52	0.98
3.53	0.77	0.84	40	62	1.00
3.77	0.78	0.85	45	70	0.98
3.99	0.78	0.85	50	78	0.98
4.40	0.78	0.87	60	94	0.98
4.80	0.81	0.88	70	114	0.98
5.78	0.83	0.89	100	166	1.00
7.16	0.84	0.92	150	252	0.98
8.52	0.90	0.93	200	360	1.00
10.51	0.93	0.94	300	560	1.02
12.18	0.93	0.95	400	740	1.00
14.28	0.95	0.95	400	1040	1.02
5.60	0.97	0.96	240	290 <sup>d</sup>	1.40 <sup>d</sup>

<sup>a</sup>  $\xi$  is the ratio of the effective decoupling bandwidth to the total sweep range.

<sup>b</sup>  $f$  is the ratio  $B_2(\text{RMS})/B_2(\text{max})$ .

<sup>c</sup>  $n$  is the exponent in the expression for the WURST pulse envelope (Eq. [12]).

<sup>d</sup> Obtained with  $J = 151$  Hz,  $m = 4.4$ ,  $Q_0 = 1.0$ ,  $T = 1.5$  ms.

The penalty for procuring very high figures of merit is a higher level of cycling sidebands (18) in the decoupled spectrum, because with high  $\Phi$  values one comes closer to violating the two essential conditions,  $J_{\text{IS}}T \ll 1$  and  $Q_0 \gg 1$ . This can seriously interfere with the detection of weak signals, for example, in two-dimensional nuclear Overhauser spectroscopy (NOESY) with isotopically labeled biological macromolecules. Some relief can be obtained by “asynchronous” decoupling—starting signal acquisition at a randomly selected point in the decoupling cycle, so that the cycling sidebands have a variable phase (13) and tend to cancel (19). A more certain remedy is to increase the sweep rate and increase the radiofrequency level, thus accepting a lower figure of merit  $\Phi$ . Fortunately, the high bandwidths attainable by WURST decoupling leave ample leeway for such adjustments.

We illustrate this question of spectral purity with a  $\{^{13}\text{C}\}$ H decoupling experiment on  $^{13}\text{C}$ -enriched sodium acetate, performed on a Varian UNITY *plus* 750 MHz spectrometer. The idea is to demonstrate the effect that cycling sidebands would have on a two-dimensional proton NOESY experiment when  $^{13}\text{C}$  synchronous decoupling is employed. The proton frequency was incremented over 2.5 kHz to simulate a strong diagonal response while the decoupler frequency was incremented over a range of 64 kHz, giving effective decoupling in the central region of  $\pm 15$  kHz. Setting the contour level at 0.2% of the maximum proton re-

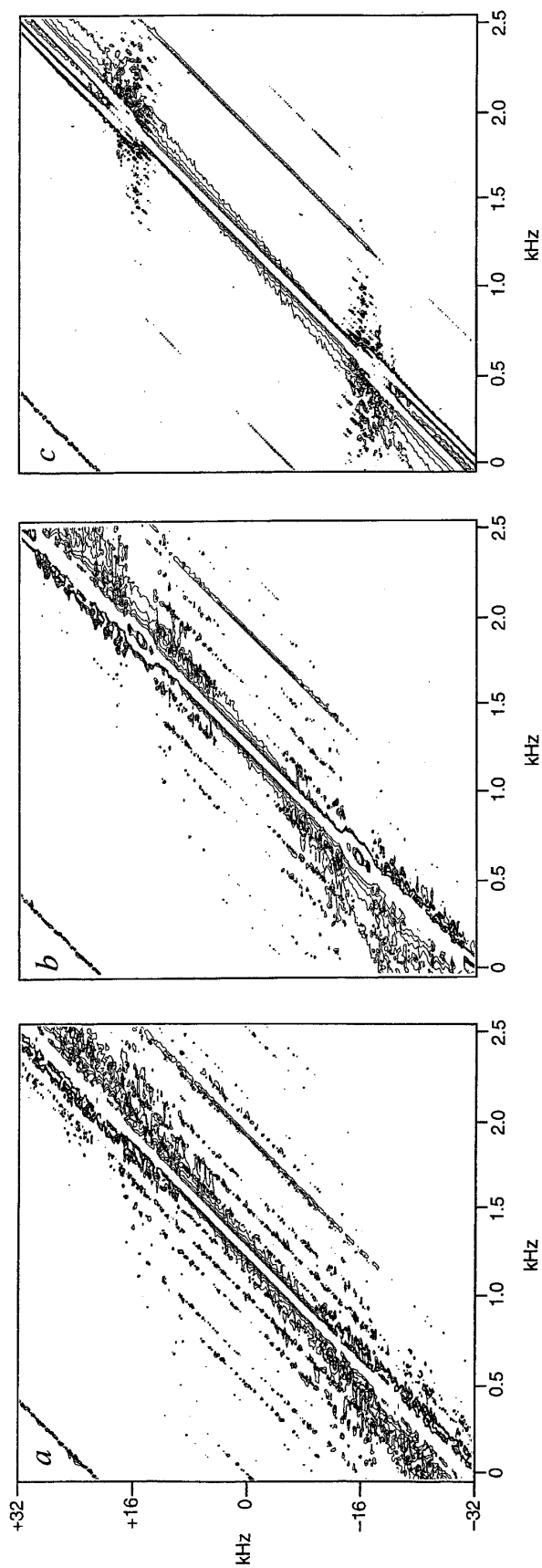


**FIG. 3.** Comparison of cycling sidebands when decoupling with (a) GARP, (b) WALTZ-16, and (c) WURST-2 under equivalent conditions, using  $^{13}\text{C}$ -enriched sodium acetate. The carrier frequency was incremented over a range of 2.5 kHz across the proton signal to create the effect of a strong diagonal response. The  $^{13}\text{C}$  decoupler frequency was incremented from  $-32$  to  $+32$  kHz and was effective over the central range of  $\pm 15$  kHz, with  $\gamma B_2(\text{RMS})/2\pi = 4$  kHz,  $Q_0 = 1.7$ , and  $T = 0.5$  ms. The contour level was set at 0.2% of the maximum decoupled response. This simulates what would be observed in a two-dimensional NOESY experiment. Small impurity peaks give rise to two resonances that run parallel to the main diagonal, on the right and in the upper left corner.

sponse highlights the cycling sidebands. The results are compared with those from WALTZ-16 (6) and GARP (7) decoupling, using the same decoupler level,  $\gamma B_2(\text{RMS})/2\pi = 4$  kHz. As expected from earlier investigations (18), GARP shows the most obtrusive cycling sidebands, WALTZ-16 provides a rather better performance, while WURST-2 gives a much higher spectral purity in the decoupled region (Fig. 3). These results were achieved by increasing the adiabaticity factor  $Q_0$  to 1.7, and by reducing the sweep duration  $T$  to 0.5 ms, giving an effective decoupling bandwidth  $\Delta F^* = 30$  kHz. The apodization of the amplitude profile was deliberately made very mild ( $n = 2$ ). These very conservative operating conditions ( $\Phi = 0.28$ ) could be used in any situation where cycling sidebands might present a problem. We conclude that adiabatic fast passage provides inherently more complete spin inversion than the composite pulses used in WALTZ-16 and GARP.

### REFERENCES

1. R. R. Ernst, *J. Chem. Phys.* 45, 3845 (1966).
2. M. H. Levitt and R. Freeman, *J. Magn. Reson.* 43, 502 (1981).
3. M. H. Levitt, R. Freeman, and T. Frenkiel, *J. Magn. Reson.* 47, 328 (1982).
4. J. S. Waugh, *J. Magn. Reson.* 50, 30 (1982).
5. M. H. Levitt, R. Freeman, and T. Frenkiel, *J. Magn. Reson.* 50, 157 (1982).
6. A. J. Shaka, J. Keeler, and R. Freeman, *J. Magn. Reson.* 53, 313 (1983).
7. A. J. Shaka, P. B. Barker, and R. Freeman, *J. Magn. Reson.* 64, 547 (1985).
8. T. Fujiwara, T. Anai, N. Kurihara, and K. Nagayama, *J. Magn. Reson. A* 104, 103 (1993).
9. Z. Starčuk, Jr., K. Bartušek, and Z. Starčuk, *J. Magn. Reson. A* 107, 24 (1994).
10. M. R. Bendall, *J. Magn. Reson. A* 112, 126 (1995).
11. Ě. Kupče and R. Freeman, *J. Magn. Reson. A* 115, 273 (1995).
12. R. Fu and G. Bodenhausen, *Chem. Phys. Lett.* 245, 415 (1995).
13. Ě. Kupče and R. Freeman, *J. Magn. Reson. A* 117, 246 (1995).
14. R. Fu and G. Bodenhausen, *J. Magn. Reson. A* 117, 324 (1995).
15. Ě. Kupče and R. Freeman, *J. Magn. Reson. A* 118, 299 (1996).
16. J. Baum, R. Tycko, and A. Pines, *Phys. Rev. A* 32, 3435 (1985).
17. R. Tycko, A. Pines, and R. Gluckenheimer, *J. Chem. Phys.* 83, 2775 (1985).
18. A. J. Shaka, P. B. Barker, C. J. Bauer, and R. Freeman, *J. Magn. Reson.* 67, 396 (1986).
19. R. Freeman, T. Frenkiel, and M. H. Levitt, *J. Magn. Reson.* 50, 345 (1982).